Improved security and stability of grid connected the wind energy conversion system by unified power flow controller

I Made Wartana[1], Ni Putu Agustini[1], Sasidharan Sreedharan[2]

[1]Department of Electrical Engineering, National Institute of Technology Malang, Malang, Indonesia
[2]Department of Electrical and Electronics Engineering, MES College of Engineering, Kuttippuram, India

Article Info

ABSTRACT

The stability and security improvements of the grid-connected to the wind energy conversion system (WECS) can be made by optimizing the placement of a flexible alternating current transmission system (FACTS). This study discusses the optimal placement of one type of WECS, namely the doubly-fed induction generator (DFIG) with a series and a shunt-FACTS control device called unified power flow controller (UPFC). The DFIG and UPFC connected grid dynamic performance improvement with a maximum load bus system scenario. The optimal placement of DFIG and UPFC on the grid is formulated as a multi-objective problem, namely maximizing load bus system (Max. LBS) while minimizing active power loss (Min. P_{loss}) by pleasing numerous security and stability constraints. The non-dominated sorting genetic algorithm II (NSGA-II) have been utilized to settle this opposed bi-objective enhancement problem. The validity of the suggested method was examined on a modified IEEE 14-bus and a utilitarian examine system connected to DFIG with UPFC in power system analysis toolbox (PSAT) software. The optimal placement of DFIG and UPFC on the grid has increased the system's dynamic performance, with all the specified particular constraints being encountered.

Corresponding Author:

I Made Wartana
Department of Electrical Engineering, National Institute of Technology (ITN)
2nd Campus, Street of Raya Karanglo Km. 2, Malang, Indonesia
Email: m.wartana@lecturer.itn.ac.id

1. INTRODUCTION

Electrical energy plants distraibute electrical power to meet consumer needs by prioritizing safety, reliability, and stability [1], [2]. Recently, conventional energy generation technology, which mainly uses coal, petroleum, and nuclear fuel, has experienced a setback due to the depleting availability of fuel oil, economic awareness, concern for environmental issues, and safety measures. Therefore, the development of efficient renewable energy conversion and utilization techniques is the main focus in the future. One of the efficient conversion techniques is wind energy because it utilizes environmentally friendly and pollution-free energy sources [3].

Therefore, the number of wind energy conversion systems (WECS) connected to the system has increased rapidly. Some problems arise due to the integration of the WECS to the grid, such as the double-fed induction generator (DFIG), and need detailed analysis in solving these problems [4]. Integrated DFIG into the grid requires installing a shunt controller to support voltage requirements and a series controller to control line flow, increasing the system's load capacity. The integrated power flow controller (UPFC) can simultaneously control line flow and voltage [5], [6]. Therefore, to solve the problem of maximizing the load bus system (Max. LBS) while reducing the active power loss (Min. P_{loss}), it is necessary to consider various

security and system stability constraints [7]. The optimal placement and settings of UPFC to minimize active power loss in an optimally integrated DFIG in the grid to maximize the load bus system need to be determined.

Numerous challenges arise due to the large-scale integration of renewable energy resources into the network to improve system performance [8], [9]. Sisay and Jately [10], to enhance the dynamic performance of grid-connected wind farms and improve the system's transmission capability, a UPFC is interconnected at the voltage at the point of mutual pairing. The use of modern UPFC integrated into the network to improve the dynamic performance of the wind farm was proposed in [11] and [12] to reduce power quality problems by increasing the transmission capability of the dynamic response system of the ac network. Liu *et al.* [13], the stability of the integrated grid system with DFIG and direct drive permanent magnet synchronous generator and UPFC was analyzed by comparing the structure, principles, and mathematical simulation models of the two wind turbines. The ant-colony optimization (ACO) and adaptive neuro fuzzy inference system (ANFIS) algorithms are proposed in [14] for the WECS and UPFC optimal reactive power delivery (ORPD) techniques in grid-connected power systems. Integrated power system using DFIG with three-phase fault using UPFC [15], whereas, Vig and Surjan [14] proposes a high-precision new grid-connected three-phase inverter system with a sub-inverter using a combination type UPFC structure consisting of a central inverter, a sub-inverter, and a transformer. The stability of DFIG and UPFC integrated into the power system on the critical clearing fault time in a multi-machine power system has been investigated in work [16].

This paper deliberates integrating WECS type DFIG, and flexible alternating current transmission system (FACTS) devices type UPFC into the network to improve network security and stability. The problem is solved by multi-objective operational control, including max. LBS strategy and min. P_{loss} by encounter several line stability and security constraints such as small-signal stability, generation limit, voltage limit, and the loading limit. To achieve this dynamic goal, simultaneously, the most versatile series and shunt-FACTS controller, UPFC, have been implemented. The optimal location and sizing of the DFIG and UPFC into the grid is formulated as a multi-objective optimization problem implemented on a modification of the IEEE 14 bus standard test system and the practical Indonesian Java-Bali 24-bus system.

2. RESEARCH METHOD
2.1. WECS modelling

The most commonly used wind energy conversion system (WECS) nowadays is DFIG since it has some advantages, working at despicable wind speed synchronous speed and regulating output power and voltage [17]. It is composed of an induction generator and a winding rotor with two converters was to inject a universal voltage into the rotor circuit at a phase shift and a varying frequency. Both converters can control in two means, either alternating current/direct current (AC/DC) (forward) or DC/AC (reverse) in this system. The rotor-connected converter and the grid-connected converter are called rotor converter and line converter, respectively. The DFIG provides flexible operating and robust control, being power can flow in both directions as per system conditions. Figure 1 shows a DFIG component model that adequately captures electromechanical dynamics described in detail [18]. As shown in (1) formulates the generator's active and reactive power production depending on the stator and converter currents and the stator and converter voltages, respectively.

$$
\left.\begin{array}{l}
p_h = v_{s,d}i_{s,d} + v_{s,q}i_{s,q} + v_{c,d}i_{c,d} + v_{c,q}i_{c,q} \\
q_h = v_{s,q}i_{s,d} - v_{s,d}i_{s,q} + v_{c,q}i_{c,d} - v_{c,d}i_{c,q}
\end{array}\right\}
\tag{1}
$$

If expression (1) is rewritten, it can be a function of the stator and rotor currents being $i_{s,d} + ji_{s,q}$ and $i_{r,d} + ji_{r,q}$, and the stator and rotor voltages $v_{s,d} + jv_{s,q}$ and $v_{r,d} + jv_{r,q}$, respectively.
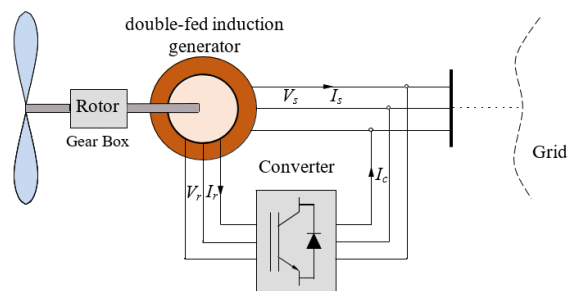

Figure 1. DFIG component modeling

2.2. UPFC modeling

This type of series and shunt FACTS controller is designed for precise timing control of the power system and dynamic compensation for undesired conditions. It can control the power flow of the system by adjusting the varied factors that influence it. Because of its ability to generate a voltage at any phase angle and independently regulate the real power flow regardless of reactive power, the UPFC is the most commonly used. However, it is relatively more expensive among various FACTS device compensation techniques [5]. The UPFC consists of a static synchronous compensator (shunt voltage source inverter (VSI)) and a series static synchronous compensator (VSI Series) coupled together via a typical DC link capacitor, providing a two-way real power exchange between the shunt and the series section as shown in Figure 2 [19], [20]. By adding shunt power and serial power insertion on buses i and j, the UPFC's basic structure and mathematical model can be formulated as shown in Figure 2(a) and Figure 2(b), respectively. While equations (2) and (3) state the equivalent power injection element [11]. How quickly and accurately the reference signal is generated will determine the performance of the UPFC where a suitable dc-link current regulator is used to establish the actual reference signal after eliminating the fluctuating signal.

$$\left.\begin{array}{l} P_{i,UPFC} = 0{,}02 r b_{se} V_i^2 \sin\gamma - 1. - 2 r b_{se} V_i V_j \sin(\theta_i - \theta_j + \gamma) \\ P_{j,UPFC} = r b_{se} V_i V_j \sin(\theta_i - \theta_j + \gamma) \end{array}\right\} \tag{2}$$

$$\left.\begin{array}{l} Q_{i,UPFC} = -r b_{se} V_i^2 \cos\gamma \\ Q_{j,UPFC} = r b_{se} V_i V_j \cos(\theta_i - \theta_j + \gamma) \end{array}\right\} \tag{3}$$
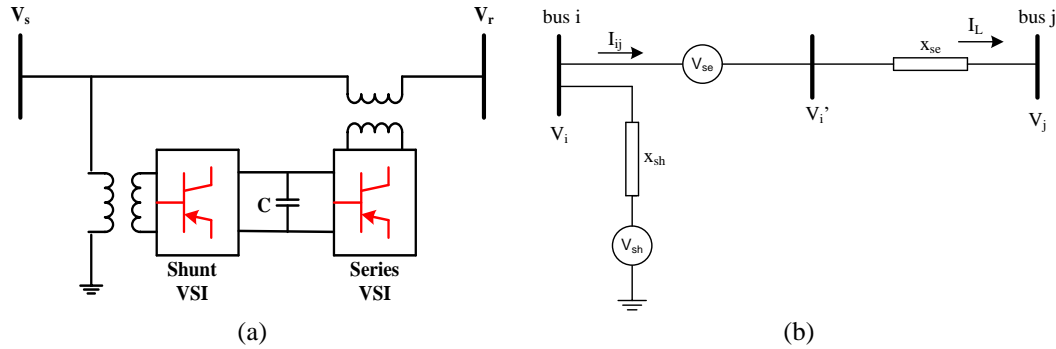

Figure 2. UPFC model in power system; (a) basic structure and (b) mathematical model

2.3. Problem formulation

This study elaborates conflicting bi-objective optimization on maximizing load bus system (Max. LBS) with minimizing active power loss (Min. P_{loss}) by pleasing numerous security and stability constraints to verify the method proposed. The optimization problem is conceivably concurrently determined by non-dominated sorting genetic algorithm II (NSGA-II), which formulates as $f(x,u)$ in (4) and (5) [21], with x and u represented dependent and control variables, respectively.

$$\text{Max.} f(\mathbf{x}, \mathbf{u}) = [f_1(\mathbf{x}, \mathbf{u}), -f_2(\mathbf{x}, \mathbf{u})] \tag{4}$$

$$\text{s.t.} : \begin{cases} g_i(\mathbf{x}, \mathbf{u}) = 0 \; i = 1, \ldots, m \\ h_j(\mathbf{x}, \mathbf{u}) \leq 0 \; j = 1, \ldots, n \end{cases} \tag{5}$$

where the bi-objective functions are represented by f_1 and f_2, with g_i being the ith equality, and h_j is the jth inequality constraints, respectively.

2.4. Maximizing load bus system (Max. LBS)

A loaded bus increase scenario λ is implemented as the primary bi-objective function in this study by Max. LBS, as shown in (6) and (7) based on the system load parameter *VL*, viz the aggregate of the thermal (OLL_i) plus bus violation limit factors (BVV_j) discussed in detail in [21].

$$Max. f_1(\mathbf{x}, \mathbf{u}, \lambda) \tag{6}$$

$$s.t. VL = \sum_{i=1}^{N_L} OLL_i + \sum_{j=1}^{N_E} BVV_j \tag{7}$$

2.5. Minimizing active power loss (Min. P_{loss})

The second objective function is Min. P_{loss} the transmission line as shown in (8) [22], [23]. The voltages on bus i and bus j of the kth line are expressed as $V_i\theta_i$ and $V_j\theta_j$, respectively. Whereas N_i is the number of transmission lines, and $g_{k(i,j)}$ is the the kth conductance.

$$\text{Min. } f_2(\boldsymbol{x}, \boldsymbol{u}) = P_{loss} = \sum_{k=1}^{N_i} g_{k(i,j)} \cdot \left[V_i^2 + V_j^2 - 2 \cdot V_i \cdot V_j \cdot \cos\theta_{ij} \right] \tag{8}$$

2.6. Equality and inequality constraints
2.6.1. Equality constraints

The equality constraints expressed in (9) are typical load flow equations where N_b is the number of buses. The active and reactive power loads are P_{Li} and Q_{Li}, respectively. Moreover G_{ij}, B_{ij} and θ_{ij} are the admittance and angle of admittance.

$$\left. \begin{array}{l} P_{G_i} = P_{L_i} + V_i \cdot \sum_{i=1}^{N_b} V_j \cdot (G_{ij} \cdot \cos\theta_{ij} + B_{ij} \cdot \sin\theta_{ij}); \\ Q_{G_i} = Q_{L_i} + V_i \cdot \sum_{i=1}^{N_b} V_j \cdot (G_{ij} \cdot \sin\theta_{ij} + B_{ij} \cdot \cos\theta_{ij}); \end{array} \right\} i = 1,2,\ldots\ldots,N_b \right\} \tag{9}$$

2.6.2. Inequality constraints

The inequality constraints in this study are active P_{Gi} and reactive power generators Q_{Gi}, voltage V_i, and phase angle θ_i (10). The parameter settings of UPFC: series voltage v_s and shunt current i_{SH} as shown in (11). Furthermore, P_{ij} in (12) is transmission loading.

$$\left. \begin{array}{l} P_{G_i}^{min} \le P_{G_i} \le P_{G_i}^{max} \\ Q_{G_i}^{min} \le Q_{G_i} \le Q_{G_i}^{max}; \\ V_i^{min} \le V_i \le V_i^{max}; \\ -0,9 \le \theta_i \le 0,9; \end{array} \right\} i = 1,2,\ldots\ldots,m \tag{10}$$

$$\left. \begin{array}{l} {}_S^{min} \le v_S \le v_S^{max} \\ i_{SH}^{min} \le i_{SH} \le i_{SH}^{max} \end{array} \right\} \tag{11}$$

$$\left| P_{ij} \right| \le P_{ij}^{max}; ij = 1,2,\ldots\ldots\ldots,N \tag{12}$$

2.7. Stability constraints
2.7.1. Small-signal stability

As shown in (13) described the state-space model of the power system intended for small signal stability analysis that formulated as a differential equations and algebraic equations (DAE) [24].

$$\left. \begin{array}{l} \dot{x} = f(x,y) \\ 0 = g(x,y) \end{array} \right\} \tag{13}$$

Where x is a vector of state variables and y is an algebraic variable, respectively. By linearizing the state-space model using the Taylor series expansion at a stable operating point (x_0, y_0), as shown in (14) [25].

$$\begin{bmatrix} \Delta\dot{x} \\ 0 \end{bmatrix} = \begin{bmatrix} \nabla_x f & \nabla_y f \\ \nabla_x g & \nabla_y g \end{bmatrix} \begin{bmatrix} \Delta x \\ \Delta y \end{bmatrix} = \begin{bmatrix} A_1 & B_1 \\ C_1 & D_1 \end{bmatrix} \begin{bmatrix} \Delta x \\ \Delta y \end{bmatrix} = [A_C] \begin{bmatrix} \Delta x \\ \Delta y \end{bmatrix} \tag{14}$$

Using the manipulation of AC, a comprehensive Jacobian matrix with linearized equations of the DAE system, the state matrix As can be calculated using (15) [26].

$$A_S = F_x - F_y G_y^{-1} G_x \tag{15}$$

The eigenvalues in the S-domain can be calculated since the matrix (15) has been fulfilled, which expresses that the system is stable if the eigenvalues of the real part are negative.

2.7.2. FVSI

Fast voltage stability index (FVSI) [27] in (16) is utilized to guarantee secure bus loading since its value is close to 1.00. One of the buses connected to the line can cause an immediate voltage drop when the amount exceeds 1.00.

$$FVSI_{ij} = \frac{4Z^2 Q_j}{V_i^2 X} < 1 \qquad (16)$$

where Z and X are the impedance and reactance of the transmission line between bus i and bus j, respectively, the reactive power that flows to bus j is Q_j, and V_i is the sending-end voltage.

2.7.3. LQP

The line stability factor (LQP) is a factor that guarantees a stable system when its value is less than 1.00 [28]. At this value, the LQP ensures that no line is overloaded under all system loading conditions. The LQP as shown in (17).

$$LQP_{ij} = 4 \cdot \left(\frac{X}{V_i^2}\right)\left(\frac{X}{V_i^2} \cdot P_i^2 + Q_j\right) < 1 \qquad (17)$$

2.8. NSGA-II, a brief description

In this study, the authors selected the NSGA-II algorithm [29] to solve the conflicting multi-objective problem as shown in (4) by finding the Pareto-optimal set. A fast non-dominant sorting approach is applied to this algorithm to find a group of equally good solutions closest to the Pareto optimal front. By calculating the crowding distance, the diversity of the Pareto-optimal solutions is maintained. Whereas allowing parental and offspring populations to participate in the competition increases the convergence nature of optimization theory, Elitism was introduced [30], [31]. Details of the procedure and critical parts of the NSGA-II method are given in [32]. A set of best solutions that fulfill multi-objectives, the best compromise solution (Best CS), is taken using a fuzzy set with full membership from the Pareto front [33].

3.   RESULTS AND DISCUSSION

In this study, the DFIG and UPFC are optimally installed on the grid to control the system's stability and security by maximizing the load bus system (Max. LBS). Investigate the Max. LBS during Min.P_{loss} is done with adequate numerous system's security and stability using the NSGA-II techniques vis: i) base case (without DFIG or UPFC); ii) case-1 (with DFIG only); iii) case-2 (with UPFC only); and iv) case-3 (with DFIG and UPFC). The effectiveness of the proposed approach for all the cases was simulated using a modified standard test system, IEEE 14-bus [34], [35], and the Indonesia Java-Bali 24-bus system as a practical test system [21], [36].

3.1. A modified standard test system, IEEE 14-bus
3.1.1. Base case (without DFIG or UPFC)

In this case, DFIG and UPFC are not connected to the grid, so all system stability is not examined. Then the system load is enhanced to obtain Max. LBS and Min. P_{loss} was 149.59% and 0.1625 p.u, respectively, as shown on the Pareto front in Figure 3. The minimum P_{loss} obtained for the best CS is slightly higher than the preceding result of 1.1704 p.u, but Max. LBS is much lower at 114.40%.
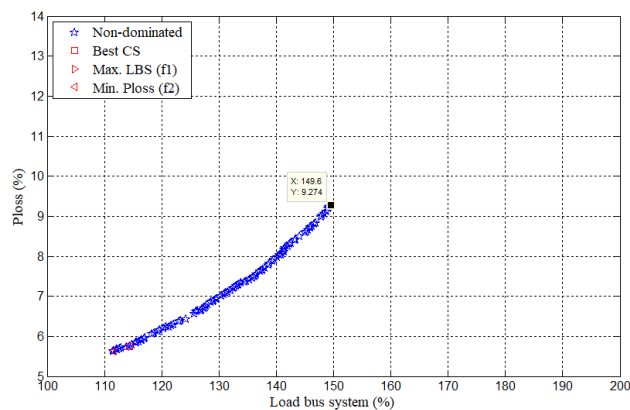

Figure 3. The base case's Pareto front

3.1.2. Case-1 (DFIG only)

In Case-1, the best CS is achieved by optimal placement of one DFIG on bus 8, with 49.91 MW and −11.56 MVAr, to carry out the best P_{loss} of 0.1772 p.u, but with the Max. LBS 112.24%, which is the lowest in Case-1, as shown in Figure 4. When placed the DFIG on bus-14, it gained the best of Max. LBS of 157.08% and P_{loss} of 0.4885 p.u. All the security and stability constraints are satisfied in this case. Moreover, a small signal that guarantees the grid's stability on the best CS is shown in Figure 5, stated by the S field's negative eigenvalues.
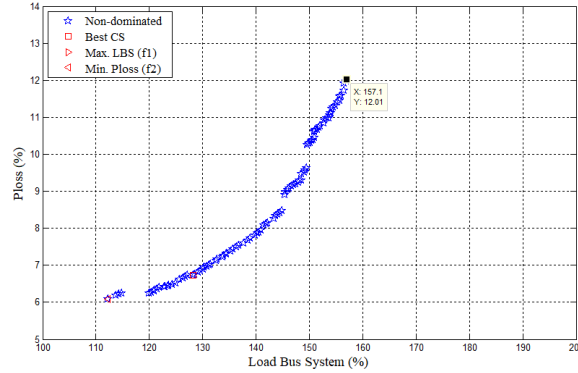
Figure 4. Case-1's Pareto front
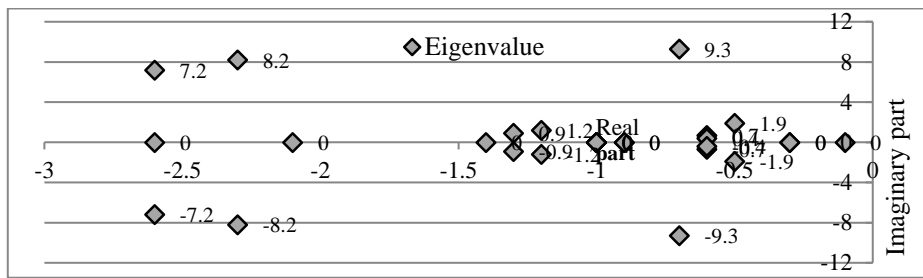
Figure 5. Case-1's Eigenvalues

3.1.3. Case-2 (UPFC only)

Figure 6 detects that by installing the UPFC at the optimal location on lines 1-5, the Pareto front appears an increase in Max. LBS extreme reached 179.25%, with P_{loss} similarly a bit high at 11.02% (0.5115 p.u.). Meanwhile, placing the UPFC on lines 9-14 with shunt and series settings of 0.412 and -13.0707 p.u., respectively, is achieved, Min. P_{loss} of 0.1911 p.u. which is the Best P_{loss} in Case-2, even though Max. LBS decreased drastically only by 118.37%. However, in Case-2, all system security and stability constraints are met for the two conditions in Figure 7.
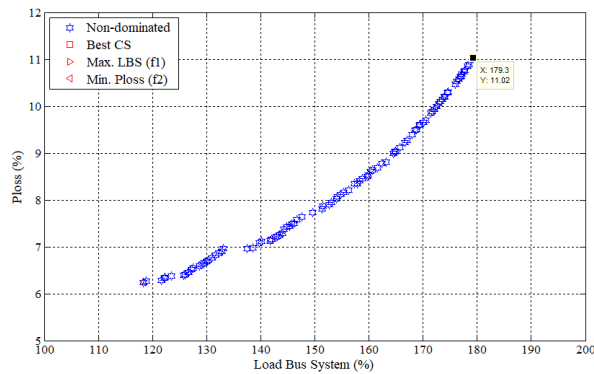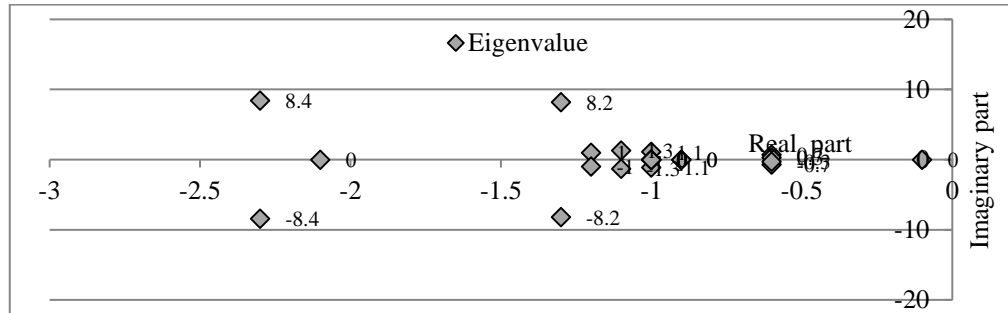

Figure 6. Case-2's Pareto front

Figure 7. Case-2's Eigenvalues

3.2. Case-3 (DFIG and UPFC)

For Case-3, by optimally installing DFIG on bus-4 and UPFC on lines 9-10 in the grid, it can be seen that there is an increase in system loading, reaching the most extreme value (Best LBS) of 193.71% with a high P_{loss} of 15.31% (0.7683 p.u) as illustrated in Figure 8. The increase was achieved with DFIG capacities of 95.37 MW and -25.89 MVar with UPFC settings of 0.5 and -60.1915 p.u, for shunt and series, respectively. Intermediate results obtained on Best CS with Max. LBS and Min. P_{loss} is 159.75 % and 0.3261 p.u, respectively, by optimal placement of DFIG with a size of 67.24 MW, -29.49 MVar on bus 14 and UPFC on lines 1-5 with shunt and series settings 0.5 and 20 p.u, respectively. Figure 9 shows that the system stability is fulfilled in Best CS, with all real parts of the eigenvalues being negative. While Figure 10 denoted the security constraints based on the FVSI and LQP for all cases in a safe condition with values less than 1.00.
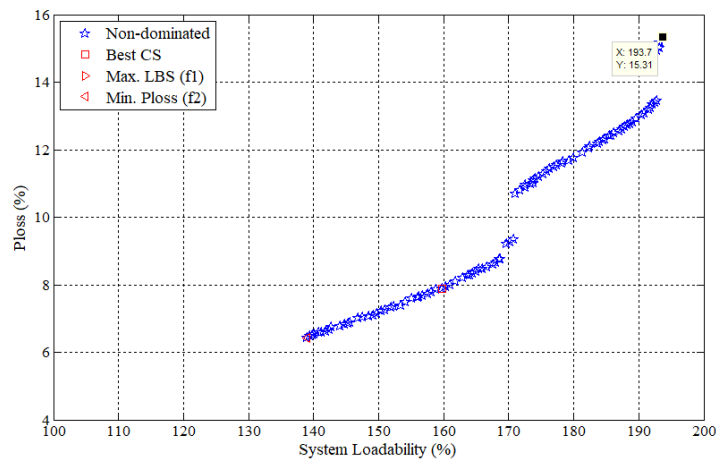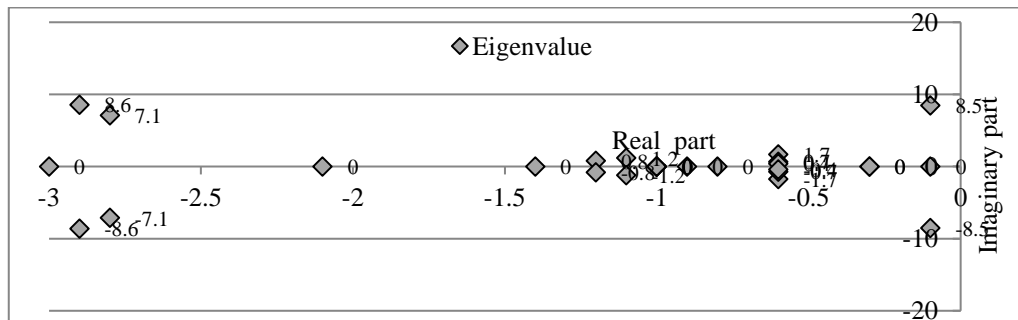

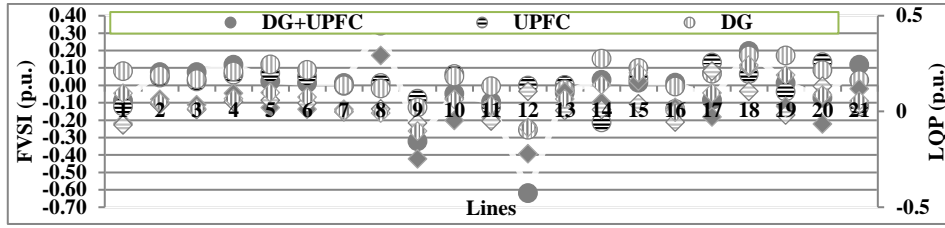Figure 8. Case-3's Pareto front

Figure 9. Case-3's Eigenvalues

Figure 10. FVSI and LQP for all Cases

3.3. A modified practical test Indonesia Java-Bali 24-bus system

A simulation has been carried out on a modified Java-Bali 24-bus Indonesian practical test system as despicted on Figure 11 [36], [37] to prove the proposed method. Figure 12 shows the Best LBS obtained at 165.87% with a P_{loss} of 2,545% (1,3480 p.u.) by the optimal installation of DFIG 138.91 MW, -62.99 MVar on bus 13 and by placing UPFC on the exact location at lines 18-19 with shunt and series settings of 1.00 and -62.99 p.u., respectively. Best CS was obtained with ploss reduced by almost half, of 2.5421 p.u. But with a decrease in Max. LBS is not too large of 144.09% compared to the previous result, with the system stability is guaranteed, as shown in Figure 13 with a negative eigenvalue. The system security is also certified for all cases for this practical test system. It is reflected in their values less than 1.00 for the FVSI and LQP indices, as shown in Figure 14.
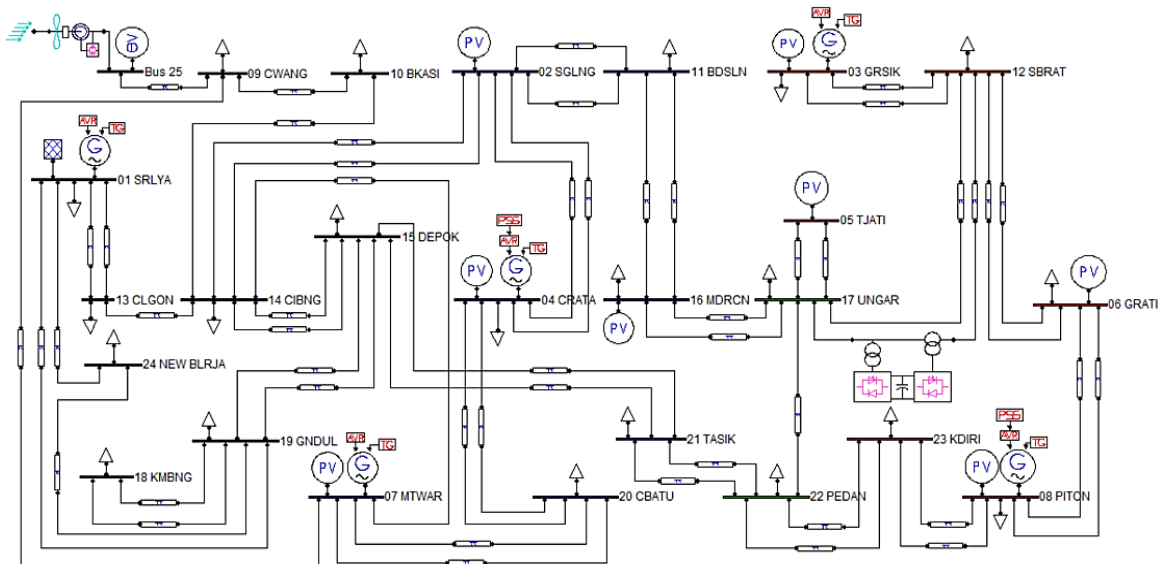

Figure 11. Single line diagram of a modified Java-Bali 24-bus Indonesia practical test system
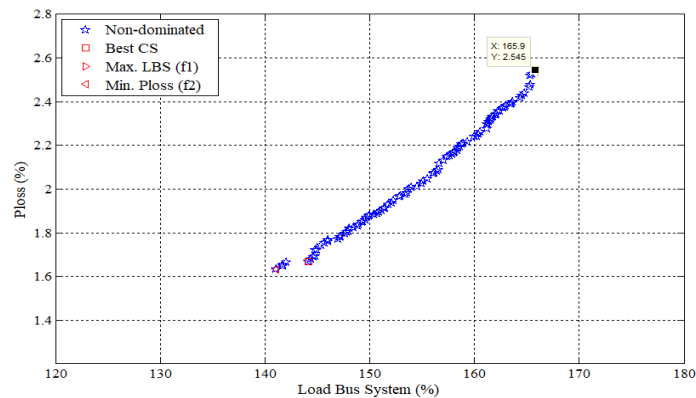

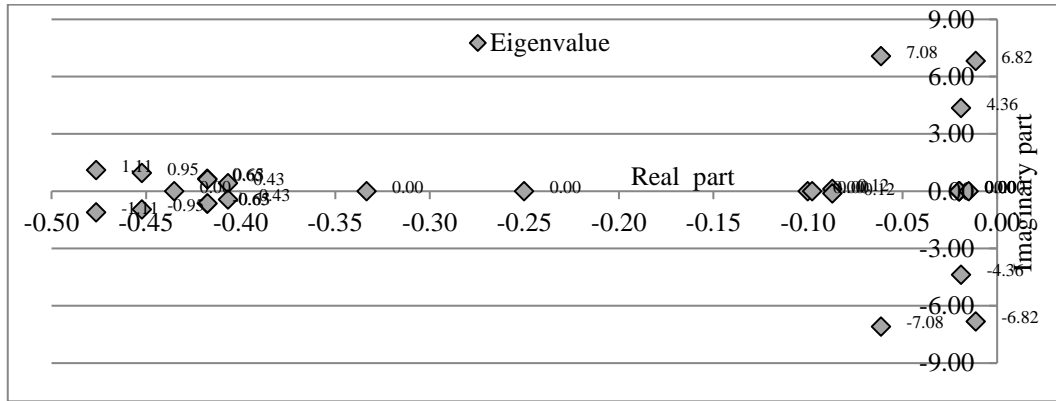Figure 12. Case-3's Pareto front of the Indonesia Java-Bali 24-bus system

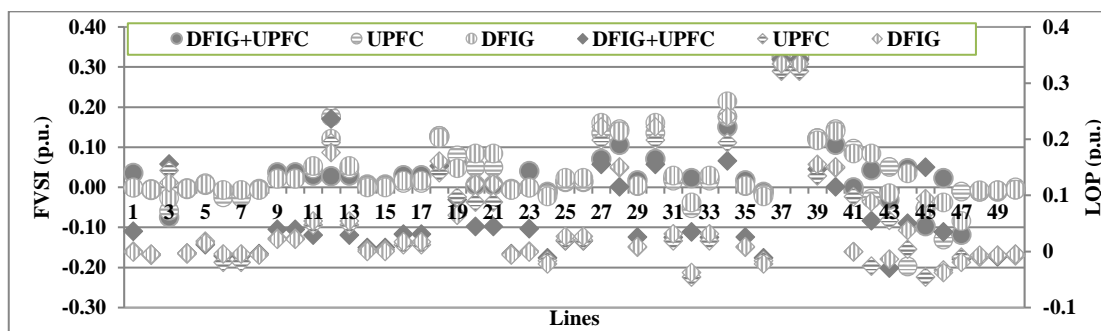Figure 13. Case-3's Eigenvalues of the Indonesia Java-Bali 24-bus system

Figure 14. FVSI and LQP of all cases for the Indonesia Java-Bali 24-bus system

4. CONCLUSION

A new method to improve system dynamic performance involving various security and system stability constraints has been successfully tested in this study with the optimal placement of DFIG and UPFC on the grid. The multiobjective issue was dealt with involving Max. LBS for Min. P_{loss} uses the NSGA-II technique, applied to standardized test systems and practical test systems to improve the security and stability of network-connected DFIG and UPFC, with all constraints satisfied. Bus voltage violation limits and line thermal limits are considered system safety constraints. Various system stability constraints were evaluated, including the voltage stability index (FVSI), the line stability factor (LQP) reaching a value of less than 1.0, and the small-signal stability expressed by its eigenvalues attaining negative values. The test results are proven by presenting the Pareto front in the best LBS (f_1) condition and the best P_{loss} (f_2) with a relatively extreme score of 193.71% and 0.2316%, respectively, for the standard 14-bus test system. At the same time, a fuzzy-based mechanism is used to obtain the best CS as an alternative to the two previously obtained conditions, which are 159.75% and 0.3261%, respectively. Because the type of FACTS used in this study is UPFC which has the most expensive investment cost among all types of FACTS devices, this research needs to be continued by considering additional objective functions to minimize FACTS costs.

REFERENCES

[1] L. Yao, X. Shi, and P. Andrews-Speed, "Conceptualization of energy security in resource-poor economies: The role of the nature of economy," *Energy Policy*, vol. 114, pp. 394–402, Mar. 2018, doi: 10.1016/j.enpol.2017.12.029.
[2] M. Daneshvar, S. Asadi, and B. Mohammadi-Ivatloo, "Overview of the grid modernization and smart grids," in *Power Systems*, 2021, pp. 1–31.

[3]   M. S. Nazir, A. J. Mahdi, M. Bilal, H. M. Sohail, N. Ali, and H. M. N. Iqbal, "Environmental impact and pollution-related challenges of renewable wind energy paradigm – A review," *Science of the Total Environment*, vol. 683, pp. 436–444, Sep. 2019, doi: 10.1016/j.scitotenv.2019.05.274.

[4]   P. K. Dash, R. K. Patnaik, and S. P. Mishra, "Adaptive fractional integral terminal sliding mode power control of UPFC in DFIG wind farm penetrated multimachine power system," *Protection and Control of Modern Power Systems*, vol. 3, no. 1, 2018, doi: 10.1186/s41601-018-0079-z.

[5]   H. Jiang *et al.*, "Application of UPFC to mitigate SSR in series-compensated wind farms," *The Journal of Engineering*, vol. 2019, no. 16, pp. 2505–2509, Mar. 2019, doi: 10.1049/joe.2018.8533.

[6]   R. Thumu, K. H. Reddy, and C. R. Reddy, "Unified power flow controller in grid-connected hybrid renewable energy system for power flow control using an elitist control strategy," *Transactions of the Institute of Measurement and Control*, vol. 43, no. 1, pp. 228–247, Jan. 2021, doi: 10.1177/0142331220957890.

[7]   M. I. Mosaad, A. Alenany, and A. Abu-Siada, "Enhancing the performance of wind energy conversion systems using unified power flow controller," *IET Generation, Transmission and Distribution*, vol. 14, no. 10, pp. 1922–1929, May 2020, doi: 10.1049/iet-gtd.2019.1112.

[8]   P. Du, R. Baldick, and A. Tuohy, "Integration of Large-scale renewable energy into bulk power systems," *Cham: Springer International Publishing*, 2017, doi: 10.1007/978-3-319-55581-2.

[9]   S. R. Sinsel, R. L. Riemke, and V. H. Hoffmann, "Challenges and solution technologies for the integration of variable renewable energy sources—a review," *Renewable Energy*, vol. 145, pp. 2271–2285, Jan. 2020, doi: 10.1016/j.renene.2019.06.147.

[10]   A. Sisay and V. Jately, "Dynamic performance of grid-connected wind farms with and without UPFC: A case study on ashagoda wind farm," in *Advances in Intelligent Systems and Computing*, vol. 989, 2020, pp. 559–568.

[11]   T. A. Sivakumar and M. M. Linda, "Improving the dynamic performance of grid connected wind farms using modern UPFC," *Microprocessors and Microsystems*, vol. 74, p. 103015, Apr. 2020, doi: 10.1016/j.micpro.2020.103015.

[12]   A. Gupta, K. K. Sharma, S. Vig, G. Kaur, and A. Sharma, "Power quality analysis of a wind energy conversion system using UPFC," in *Green Information and Communication Systems for a Sustainable Future*, 2020, pp. 143–158, doi: 10.1201/9781003032458-8.

[13]   H. Liu, X. Li, G. Qin, and S. Hao, "Stability of grid connected system of two types of wind turbines with UPFC," *The Journal of Engineering*, vol. 2017, no. 13, pp. 2178–2183, Jan. 2017, doi: 10.1049/joe.2017.0716.

[14]   S. Vig and B. S. Surjan, "Optimal power dispatch of WECS and UPFC with ACO and ANFIS algorithms," *International Journal on Electrical Engineering and Informatics*, vol. 10, no. 1, pp. 14–36, Mar. 2018, doi: 10.15676/ijeei.2018.10.1.2.

[15]   P. Suthar, U. Gupta, and D. K. Yadav, "Fault compensation of DFIG based integrated power system using UPFC," in *2019 2nd International Conference on Power Energy Environment and Intelligent Control, PEEIC 2019*, Oct. 2019, pp. 270–274, doi: 10.1109/PEEIC47157.2019.8976620.

[16]   D. E. Tourqui, M. Benakcha, and T. Allaoui, "Improving the electrical stability by wind turbine and UPFC," in *Lecture Notes in Networks and Systems*, vol. 35, 2018, pp. 121–132, doi: 10.1007/978-3-319-73192-6_13.

[17]   B. Mehta, P. Bhatt, and V. Pandya, "Small signal stability analysis of power systems with DFIG based wind power penetration," *International Journal of Electrical Power and Energy Systems*, vol. 58, pp. 64–74, Jun. 2014, doi: 10.1016/j.ijepes.2014.01.005.

[18]   C. Zhang, D. Ke, Y. Sun, C. Y. Chung, J. Xu, and F. Shen, "Coordinated supplementary damping control of DFIG and PSS to Suppress inter-area oscillations with optimally controlled plant dynamics," *IEEE Transactions on Sustainable Energy*, vol. 9, no. 2, pp. 780–791, Apr. 2018, doi: 10.1109/TSTE.2017.2761813.

[19]   J. Li, F. Liu, Z. Li, S. Mei, and G. He, "Impacts and benefits of UPFC to wind power integration in unit commitment," *Renewable Energy*, vol. 116, pp. 570–583, Feb. 2018, doi: 10.1016/j.renene.2017.09.085.

[20]   P. He, S. A. Arefifar, C. Li, F. Wen, Y. Ji, and Y. Tao, "Enhancing oscillation damping in an interconnected power system with integrated wind farms using unified power flow controller," *Energies*, vol. 12, no. 2, p. 322, Jan. 2019, doi: 10.3390/en12020322.

[21]   I. M. Wartana and N. P. Agustini, "Application of voltage and lines stability index for optimal placement of wind energy with a system load increase scenario," *Current Alternative Energy*, vol. 3, no. 1, pp. 44–49, Nov. 2019, doi: 10.2174/2405463103666190724105814.

[22]   M. EL-Azab, W. A. Omran, S. F. Mekhamer, and H. E. A. Talaat, "A probabilistic multi-objective approach for FACTS devices allocation with different levels of wind penetration under uncertainties and load correlation," *International Journal of Electrical and Computer Engineering*, vol. 10, no. 4, pp. 3898–3910, 2020, doi: 10.11591/ijece.v10i4.pp3898-3910.

[23]   H. Yapici and N. Çetinkaya, "An improved particle swarm optimization algorithm using eagle strategy for power loss minimization," *Mathematical Problems in Engineering*, vol. 2017, pp. 1–11, 2017, doi: 10.1155/2017/1063045.

[24]   P. Dey, A. Bhattacharya, and P. Das, "Tuning of power system stabilizer for small signal stability improvement of interconnected power system," *Applied Computing and Informatics*, vol. 16, no. 1–2, pp. 3–28, Dec. 2017, doi: 10.1016/j.aci.2017.12.004.

[25]   J. Bhukya and V. Mahajan, "Integration of DFIG based wind turbine generator on small signal stability of power systems," in *2017 Innovations in Power and Advanced Computing Technologies, i-PACT 2017*, Apr. 2017, vol. 2017-January, pp. 1–6, doi: 10.1109/IPACT.2017.8244971.

[26]   I. M. Wartana, N. P. Agustini, and J. G. Singh, "Optimal integration of the renewable energy to the grid by considering small signal stability constraint," *International Journal of Electrical and Computer Engineering (IJECE)*, vol. 7, no. 5, p. 2329, Oct. 2017, doi: 10.11591/ijece.v7i5.pp2329-2337.

[27]   S. H. E. Osman, G. K. Irungu, and D. K. Murage, "Application of FVSI, Lmn and CPF techniques for proper positioning of FACTS devices and SCIG wind turbine integrated to a distributed network for voltage stability enhancement," *Engineering, Technology & Applied Science Research*, vol. 9, no. 5, pp. 4824–4829, Oct. 2019, doi: 10.48084/etasr.3101.

[28]   N. P. Agustini, L. M. Hayusman, T. Hidayat, and I. M. Wartana, "Security and stability improvement of power system due to interconnection of DG to the grid," *Lecture Notes in Electrical Engineering*, vol. 365, pp. 227–237, 2016, doi: 10.1007/978-981-287-988-2_24.

[29]   K. Deb, S. Agrawal, A. Pratap, and T. Meyarivan, "A fast elitist non-dominated sorting genetic algorithm for multi-objective optimization: NSGA-II," in *Lecture Notes in Computer Science (including subseries Lecture Notes in Artificial Intelligence and Lecture Notes in Bioinformatics)*, vol. 1917, pp. 849–858, 2000, doi: 10.1007/3-540-45356-3_83.

[30]   A. K. Singh and S. K. Parida, "A multiple strategic evaluation for fault detection in electrical power system," *International Journal of Electrical Power and Energy Systems*, vol. 48, no. 1, pp. 21–30, Jun. 2013, doi: 10.1016/j.ijepes.2012.11.033.

[31]   M. B. Shadmand and R. S. Balog, "Multi-objective optimization and design of photovoltaic-wind hybrid system for community smart DC microgrid," *IEEE Transactions on Smart Grid*, vol. 5, no. 5, pp. 2635–2643, Sep. 2014, doi: 10.1109/TSG.2014.2315043.

[32] S. Wang, D. Zhao, J. Yuan, H. Li, and Y. Gao, "Application of NSGA-II Algorithm for fault diagnosis in power system," *Electric Power Systems Research*, vol. 175, p. 105893, Oct. 2019, doi: 10.1016/j.epsr.2019.105893.

[33] K. Mahesh, P. Nallagownden, and I. Elamvazuthi, "Advanced Pareto front non-dominated sorting multi-objective particle swarm optimization for optimal placement and sizing of distributed generation," *Energies*, vol. 9, no. 12, p. 982, Nov. 2016, doi: 10.3390/en9120982.

[34] F. Milano, "An open source power system analysis toolbox," I*EEE Transactions on Power Systems*, vol. 20, no. 3, pp. 1199–1206, Aug. 2005, doi: 10.1109/TPWRS.2005.851911.

[35] R. D. Zimmerman, C. E. Murillo-Sánchez, and R. J. Thomas, "MATPOWER: Steady-state operations, planning, and analysis tools for power systems research and education," *IEEE Transactions on Power Systems*, vol. 26, no. 1, pp. 12–19, Feb. 2011, doi: 10.1109/TPWRS.2010.2051168.

[36] I. M. Wartana, "A multi-objective problems for optimal integration of the DG to the grid using the NSGA-II," in *14th International Conference on QiR (Quality in Research), QiR 2015 - In conjunction with 4th Asian Symposium on Material Processing, ASMP 2015 and International Conference in Saving Energy in Refrigeration and Air Conditioning, ICSERA 2015*, Aug. 2016, pp. 106–110, doi: 10.1109/QiR.2015.7374906.

BIOGRAPHIES OF AUTHORS

I Made Wartana received a B.Eng. and an M.Eng. from the Electrical Engineering Department, National Institute of Technology (ITN) Malang, East Java, Indonesia and the Bandung Institute of Technology (ITB), West Java, Indonesia, in 1986 and 1994, respectively. He has been a lecturer at ITN Malang, Indonesia, since 1992. He also received a Dr. Eng. from the Asian Institute of Technology (AIT), Thailand, in 2017. His research interests include the application of FACTS controllers to the power grid, the application of AI to power systems, and the integration of renewable energies with the grid. He can be contacted at email: m.wartana@lecturer.itn.ac.id.

Ni Putu Agustini received a B.Eng. and an M.Eng. from the Electrical Engineering Department, National Institute of Technology (ITN) Malang, East Java, and Indonesia and Brawijaya University (UB), East Java, Indonesia, in 1986 and 2008, respectively. She has been a lecturer at ITN Malang, Indonesia, since 2004. Her research interests include integrating renewable energy into the power grid and the application of reliability to power systems. She can be contacted at email: ni.putu.agustini@lecturer.itn.ac.id.

Dr. Sasidharan Sreedharan received an M.Tech. in Electrical Power Systems from the Govt Engineering College, Thrissur, Kerala, India in 1998, and a Ph.D. from the Asian Institute of Technology, Bangkok, in 2010. He was a post-doctoral research fellow at the RED Lab, Renewable Energy Design Laboratory, University of Hawaii, United States, from 2014 to 2015. His research interests include the grid integration of renewable energies, the application of AI to power systems, and the stability of the grid. He can be contacted at email: sasisreedar@gmail.com.